Electromelting of Confined Monolayer Ice

Hu Qiu and Wanlin Guo*

State Key Laboratory of Mechanics and Control of Mechanical Structures and the Key Laboratory for Intelligent Nano Materials and Devices of MOE, Institute of Nano Science, Nanjing University of Aeronautics and Astronautics, Nanjing 210016, China

(Received 13 August 2012; revised manuscript received 18 December 2012; published 6 May 2013)

In sharp contrast to the prevailing view that electric fields promote water freezing, here we show by molecular dynamics simulations that monolayer ice confined between two parallel plates can melt into liquid water under a perpendicularly applied electric field. The melting temperature of the monolayer ice decreases with the increasing strength of the external field due to the field-induced disruption of the water-wall interaction induced well-ordered network of the hydrogen bond. This electromelting process should add an important new ingredient to the physics of water.

DOI: 10.1103/PhysRevLett.110.195701 PACS numbers: 64.70.dj, 61.20.Ja, 68.18.Fg

A phase transition between liquid and solid water is of fundamental importance in environmental, biological, and industrial technologies. Although the normal freezing point of bulk water is 0 °C, extremely pure liquid water cannot freeze even when cooled down to −40 °C [1]. The reason is that the high activation energy for homogeneous nucleation impedes the spontaneous formation of a stable seed nucleus for crystallization. It has been widely reported that the crystallization of liquid bulk water into cubic ice can be promoted by electric fields, so-called electrofreezing [2–6]. Freezing to a crystalline phase can also occur spontaneously when water is subjected to an extremely confined state. A number of computational [7–10] and experimental [11] studies have demonstrated the spontaneous freezing of few-layer ice confined between two parallel plates separated by nanometer gaps. Thus, it is thermodynamically more favorable to apply external electric fields to freeze liquid water confined within a nanogap [12–14] or absorbed at charged surfaces [15] due to the confinement-reduced translational entropy of water. All these theoretical simulations and experimental facts form a prevailing view that electric fields always promote the freezing of both the bulk and confined water through electric-field-induced realignment of the dipoles of water molecules. However, how an applied electric field plays its role in the reverse process to freezing (i.e., ice melting) has never been reported.

In this Letter, we show by molecular dynamics (MD) simulations that the confined monolayer ice can melt into liquid water under a perpendicularly applied electric field. The melting temperature of the monolayer ice can be significantly reduced by stronger electric fields. This unexpected electric-field-induced melting of ice, which can be named as electromelting, is mainly due to the interruption of the ordered hydrogen-bond (H-bond) network between water molecules under the perpendicular electric field.

The simulation system consists of 778 water molecules confined between two parallel plates with an area of $\sim 7.4 \times 7.4$ nm^2 along the x-y plane separated by a distance d, as measured between the centers of plate atoms (Fig. 1, bottom inset). The plates consist of a triangular arrangement of monolayer atoms, with the neighboring bond length being fixed at 0.23 nm. It has been shown that accounting for the polarizability of water in MD simulations under electric fields can affect the position of the phase boundary, but does not change the existence of each water phase in the phase diagram [16], so the nonpolarizable TIP5P model [17] will be used in our simulations without a specific statement. Although it was proposed that molecules in bulk water can be

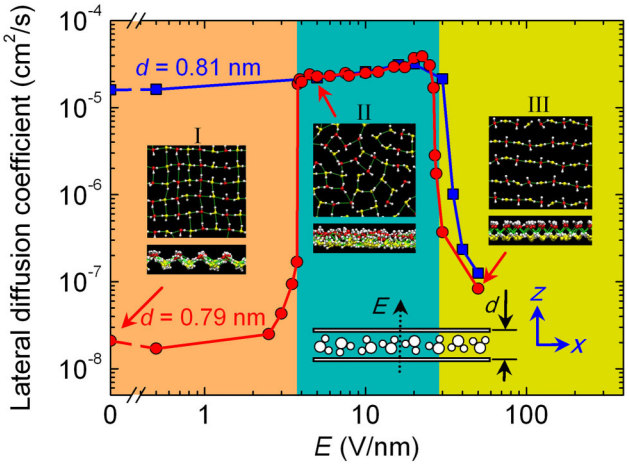

FIG. 1 (color online). In-plane diffusion coefficient of water at 300 K as a function of the external electric field (E) at two interplate spacings, $d = 0.79$ (red circle) and 0.81 nm (blue box). The bottom inset schematically shows the simulation setup. For $d = 0.79$ nm, the two confining plates are located at $z = 0.395$ and $z = -0.395$ nm, respectively. The top insets (I–III) show the in-plane and out-of-plane views of an ice monolayer at $E = 0$, a liquid water phase at $E = 5$ V/nm, and a crystal-like water phase at $E = 50$ V/nm. White atoms represent hydrogen, while red and yellow atoms represent oxygen located above and below the midplane parallel to the confining plates, respectively. H bonds are indicated by green lines.

instantaneously dissociated by electric fields ranging from 3.5 to 10 V/nm [18], our density functional theory calculations show that such dissociation cannot occur in our confined system under the perpendicularly applied electric fields [19]. The water-wall interactions were treated by a 6–12 Lennard-Jones potential with the parameters: $\sigma_{(\text{O-wall})} = 0.316\,\text{nm}$, $\sigma_{(\text{H-wall})} = 0.284$ nm and $\epsilon_{(\text{O-wall})} = 0.831$ kJ/mol, $\epsilon_{(\text{H-wall})} = 0.415$ kJ/mol. These parameters correspond approximately to the van der Waals interaction between a water molecule and a quartz (SiO_2) surface [7,8]. Periodic boundary conditions were applied in the x and y directions to model the confinement between two infinite plates, and a large vacuum layer along the z direction was used to separate adjacent images of the simulation system to avoid any unphysical interactions. The MD simulations were performed using a time step of 2 fs with the GROMACS 4.0.5 software package [20]. When the electric field was weaker than 5 V/nm, the $NP_{xy}T$ ensemble was adopted, with the Berendsen algorithm [21] being used to control the temperature T at 300 K and the lateral pressure P_{xy} at 1 bar. For stronger electric fields, the NVT ensemble was used instead to prevent the water molecules from leaving the confined area via the gap induced by the possible mismatch between the fixed confining plates and the expansible periodic simulation box along the x-y plane. The lateral pressure P_{xy} for liquid water is found to be nearly constant in NVT simulations with the increase of the field strength up to 26.5 V/nm [19]. The nonbonded interactions were treated with a twin range cutoff of 0.9 and 1.4 nm. All the other simulation parameters were the same as those used in Refs. [7,8]. Under a given electric field, the system was equilibrated for 2 ns, and then the system evolved for 8 ns for data analysis. As adopted in previous simulations [2–6,13,14], the field strength used in our MD simulations is from several V/nm to several tens of V/nm. This range of the field is at least 1×10^3 stronger than the external fields applied in electrofreezing experiments [12], but comparable to those experienced by water molecules near the surfaces of certain types of biopolymers [22] or within cracks in amino acid crystals [23]. In our model, two water molecules were considered to form a H bond if their O $\cdots$ O distance was shorter than 0.35 nm and simultaneously if the angle O-H $\cdots$ O was larger than 150°.

Previous MD simulations have shown that both monolayer ice and liquid water can form at room temperature between two plates dependent on their separating distances d [7]. The solidification of nanoconfined water was also observed experimentally at room temperature [11,24]. Consistent with the previous MD study [7], our simulation results suggest that the lateral diffusion coefficient of the monolayer ice at $d = 0.79$ nm (red circle) is about 3 orders lower in magnitude than the liquid water at $d = 0.81$ nm (blue box) in the absence of electric fields ($E = 0$ in Fig. 1). When a perpendicular electric field E is applied, the mobility of the monolayer ice remains nearly unchanged for $E < 2.5$ V/nm (see inset I in Fig. 1), with the lateral diffusion coefficient fluctuating slightly in the order of 10^{-8} cm^2/s. When the electric field enters the range of $2.5 \leq E \leq 3.75$ V/nm, the diffusion coefficient of the monolayer ice increases more and more quickly with increasing E. When the electric field approaches 3.8 V/nm, a sudden jump occurs in the lateral diffusion coefficient of the monolayer at spacing $d = 0.79$ nm from the order of $\sim 10^{-7}$ cm^2/s to the order of $\sim 10^{-5}$ cm^2/s, merging with that of the liquid water at spacing $d = 0.81$ nm. This sudden jump in diffusion coefficient means that the monolayer ice melts into a liquid state (i.e., electromelting), as also shown by inset II in Fig. 1. In the range of $3.8 \leq E < 25$ V/nm, the system at spacing $d = 0.79$ nm represents a stable liquid configuration. In comparison, the water layer between plates at spacing $d = 0.81$ nm remains in its liquid state in the whole range of $0 \leq E < 30$ V/nm. Further increasing E will lead to a sharp drop in the diffusion coefficient profiles for both plate separations, indicating a transition into a specific crystal-like structure, as shown by inset III in Fig. 1 at $E = 50$ V/nm, which exhibits strongly reduced translational and rotational dynamics with enhanced structural order [25]. The critical field strength for this liquid-to-crystal transition slightly over 35 V/nm at spacing $d = 0.81$ nm is somewhat stronger than that at spacing $d = 0.79$ nm, at about 27 V/nm. It is interesting that a similar electric-field-induced liquid-to-crystal transition can also occur in bulk water at a critical field strength of 30–40 V/nm [5,6]. To check the reliability of the TIP5P water model, we further conducted a series of MD simulations with the TIP4P water model [26]. The yielded diffusion coefficient profile in Ref. [19] exhibits a similar behavior of the phase transition, even though the detailed value of the critical field strength shows some difference, indicating the robustness of the demonstrated trend of phase transitions.

The three above demonstrated water phases exhibit distinguishing structural features, as shown by Fig. 2. Figures 2(a) and 2(b) show the transverse distributions of the density of oxygen and hydrogen atoms, respectively, at $d = 0.79$ nm under different fields. Without electric fields, water molecules in the ice monolayer confined between the two plates take a puckered structure with their oxygen atoms waving between two planes at $z \approx \pm 0.0775$ nm connected by H bonds, as shown by Fig. 2(a) and the upper panel of Fig. 2(c). This unique symmetric distribution of layered water about the middle plane at $z = 0$ is mainly attributed to the ordering effect caused by the water-wall interaction. When an external field of 5 V/nm is applied, both the planes are dragged downward approaching the lower confining plate, but the downward displacement of the lower oxygen plane (~ 0.0225 nm) is about 9 times of that of the upper oxygen plane (~ 0.0025 nm), as shown by the lower panel in Fig. 2(c). This electric-field-induced

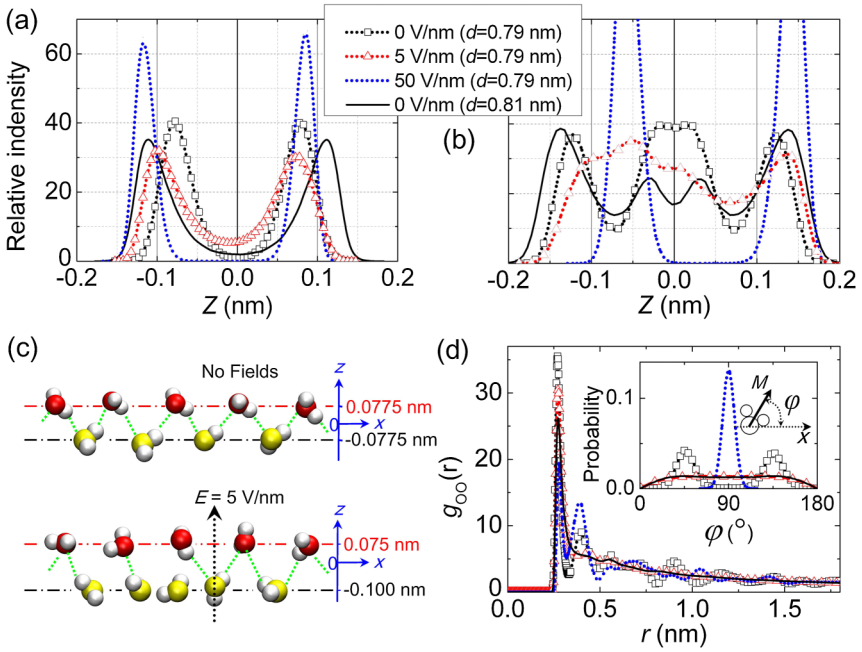

FIG. 2 (color online). Dynamics of confined water under different fields. (a), (b) Transverse distribution of the density of (a) oxygen and (b) hydrogen atoms. (c) Schematic of the increased spacing between the two water oxygen planes caused by an electric field of 5 V/nm (bottom panel) compared to the field-free case (top panel). The color representation is the same as that given in the top inset in Fig. 1. Red and black dash-dotted lines indicate the central positions of the upper oxygen plane and lower oxygen plane, respectively. (d) Oxygen-oxygen radial distribution function $g_{OO}(r)$. Inset: Probability distribution for angle φ between water molecule dipole orientation $\mathbf{M}$ and the x axis.

shift leads to a 12.9% increment in the spacing between the two oxygen planes. The detailed hydrogen distribution profiles at different fields are presented in Fig. 2(b). For the solid phase in the field-free state at $E = 0$, similar to the oxygen distribution, the hydrogen atoms are also located symmetrically with respect to the middle plane of $z = 0$. When an external field of 5 V/nm is applied, the liquid water completely loses the water-wall interaction induced symmetry in hydrogen distribution, as water molecules tend to point their hydrogen atoms upward in response to the electric field (see also inset II in Fig. 1).

We then further explored the structural properties of the monolayer ice and the electric-field-induced liquid water by examining their oxygen-oxygen radial distribution functions g_{OO} of water shown in Fig. 2(d). In the field-free case of $E = 0$, the well-defined density maxima and minima validate the high structural order of the ice phase, in which each water molecule exhibits a small amplitude fluctuation around its fixed position (see also inset I of Fig. 1). When an electric field of $E = 5$ V/nm is applied, the system loses its long-range structural order and changes into a liquid phase, as indicated by the decreased height of the second and third peaks of g_{OO}. The inherent structure of this liquid phase shows a disordered H-bond network (see also the inset II of Fig. 1). This electromelting of the confined monolayer ice can be further verified by the probability distribution of the orientation angle φ of the water molecule dipole to the x axis, as shown in the inset of Fig. 2(d). In the field-free case, there is a clear dipole orientation preference with two peaks ($\varphi = 45°$ and 135°) for the monolayer ice due to the confinement of the walls. At $E = 5$ V/nm, there is no evident peak in the φ distribution profile, confirming the loss of structural order. It should be noted that a significant discrepancy exists between the density profiles for the electric-field-induced liquid water at $d = 0.79$ nm [red dotted lines in Figs. 2(a) and 2(b)] and that at $d = 0.81$ nm in the field-free state [black solid lines in Figs. 2(a) and 2(b)], indicating that their inherent configurations are not the same. However, the nearly identical structural disorder of them, as indicated by the similar radial distribution function and φ distributions [red dotted lines and black solid lines in Fig. 2(d)], clearly shows their common liquid water nature.

The process of electric-field-induced symmetry breaking of the confined water between the two walls can be reflected more directly by monitoring the change in oxygen-wall distance with respect to the electric field as shown in Fig. 3(a), where the distance D_1 between the upper oxygen plane and wall and D_2 between the lower oxygen plane and wall, as well as their difference $D_1 - D_2$ are presented as a function of the applied electric field. For a weak electric field with $E \leq 3.75$ V/nm, the symmetric structure of confined water remains nearly unchanged with $D_1 \approx D_2 \approx 0.3175$ nm and $D_1 - D_2 \approx 0$. Although D_1 remains constant until $E = 4$ V/nm, a sharp drop in D_2

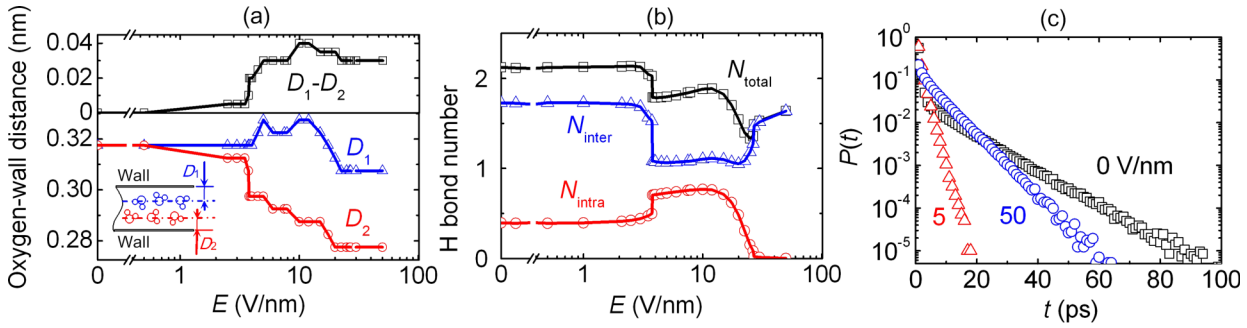

FIG. 3 (color online). Mechanism for electromelting. (a) Calculated distance between the water oxygen plane and the confining wall as a function of the electric field. (b) Average number of H bonds formed by a water molecule with other water molecules within the same plane (N_{intra}), and by a water molecule with the water molecules in another plane (N_{inter}) as a function of the electric field, together with their sum (N_{total}). (c) Probability distribution $P(t)$ of the H-bond lifetime for different field strengths.

occurs at $E = 3.8$ V/nm, breaking the symmetry with a significant increase in $D_1 - D_2$. The evolution of the structural order of confined water with an increasing field determined by the competition between the water-wall interaction and the applied electric field can be further explored by counting the average number of H bonds formed by a water molecule with its neighboring water molecules in the same oxygen plane, N_{intra}, and the average number of H bonds formed by a water molecule with the water molecules in another oxygen plane, N_{inter}, as shown in Fig. 3(b). It is found that both N_{intra} and N_{inter}, as well as their sum N_{total}, are almost constant for $E \leq 3.75$ V/nm around 0.4, 1.7, and 2.1, respectively, which is consistent with the range of the electric field for the ice phase as shown in Fig. 1. When E is further increased to 3.8 V/nm, a large sudden drop in N_{inter} and a smaller sharp jump in N_{intra} occur, resulting in a small drop in N_{total}. The large drop in N_{inter} suggests that the interplane H bonds of the monolayer ice are largely interrupted by the strong electric field, leading to the transition to the liquid phase. It is also found that after the transition the two numbers (N_{intra} and N_{inter}) in the liquid phase become closer to each other than in the monolayer ice [Fig. 3(b)], further confirming the loss of structural order of the system. Figure 3(c) shows the probability distribution $P(t)$ of the lifetime of the H bonds under different electric fields. It is found that $P(t)$ in the liquid water at $E = 5$ V/nm decays significantly faster than that in the ice phase at $E = 0$. This further suggests that the electromelting is due to the electric-field-induced breaking of the symmetric distribution and structural order of confined water determined by the water-wall interaction. It was widely believed that the favorable energetic interactions of electric fields with the dipole moments of water molecules can reduce the entropy of liquid water due to the electric-field-induced restriction of the orientational degrees of freedom [13]. If the entropy reduction is large enough, water would transform to a crystalline phase (i.e., electrofreezing), as has been demonstrated in a computer simulation of confined liquid water under an external field applied in a direction parallel to the confining plates [13]. In contrast, under external fields with similar strengths but perpendicular to the confining plates, what we demonstrate here is indeed an electric-field-induced melting (electromelting) process involving an increase in entropy. Thus, the perpendicular external electric fields applied here do not help to align the dipoles of water molecules to stabilize the H-bond network, but rather, to break the structural order caused by the water-wall interaction and lead to the ice-to-liquid transition.

The dependence of the electromelting point, namely, the temperature at which the melting occurs at a given electric field, should be an interesting and important issue to be investigated. Figure 4 presents our calculated temperature dependence of the lateral diffusion coefficient at various field strengths. In the field-free case, a sharp jump in the diffusion coefficient of the system at $T_m = 325$ K indicates that it melts into a liquid phase at this critical temperature, yielding the melting point. With increasing field strength, the electromelting point decreases gradually from 325 K at $E = 0$ to about 275 K at $E = 5$ V/nm, as shown by the inset of Fig. 4.

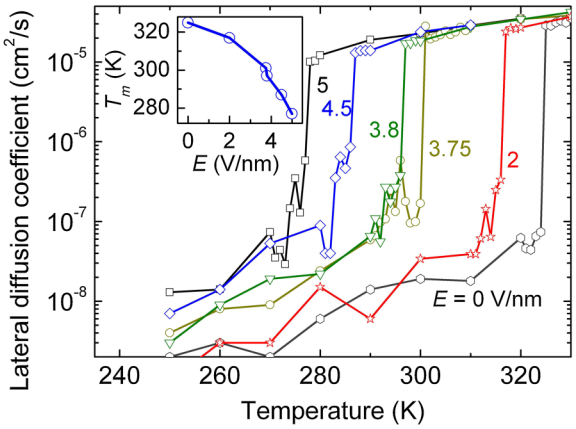

FIG. 4 (color online). Temperature dependence of the in-plane diffusion coefficient of the confined water at $d = 0.79$ nm for different external fields E. The inset shows the melting point T_m as a function of E.

In conclusion, we find an unexpected electric-field-induced melting of confined monolayer ice by comprehensive MD simulations. The critical melting temperature decreases with increasing field strength due to the field-induced reduction in the probability of H-bond formation between the water molecules in different oxygen planes forming the monolayer ice. This melting process is attributed to the success for the electric-field-induced disordering in competition with the strong water-wall interaction induced ordering of the confined water. This novel phase transition process, which can be referenced as electromelting, is in sharp contrast to the well-known electrofreezing of water and should be important for understanding the behavior of confined water.

We are grateful to Professor Yufeng Guo, Dr. Zhuhua Zhang, and Dr. Rong Shen for discussions. This work is supported by the 973 Program (No. 2012CB933403) and the national NSF Grants (No. 30970557, No. 91023026) of China, and the Funding of the Jiangsu Innovation Program for Graduate Education (CXLX11_0172), and the Fundamental Research Funds for the Central Universities.

*wlguo@nuaa.edu.cn

[1] E. B. Moore and V. Molinero, Nature (London) **479**, 506 (2011).
[2] I. M. Svishchev and P. G. Kusalik, Phys. Rev. Lett. **73**, 975 (1994).
[3] I. M. Svishchev and P. G. Kusalik, J. Am. Chem. Soc. **118**, 649 (1996).
[4] I. Borzsak and P. T. Cummings, Phys. Rev. E **56**, R6279 (1997).
[5] G. Sutmann, J. Electroanal. Chem. **450**, 289 (1998).
[6] X. Hu, N. Elghobashi-Meinhardt, D. Gembris, and J. C. Smith, J. Chem. Phys. **135**, 134507 (2011).
[7] R. Zangi and A. E. Mark, Phys. Rev. Lett. **91**, 025502 (2003).
[8] R. Zangi and A. E. Mark, J. Chem. Phys. **119**, 1694 (2003).
[9] K. Koga and H. Tanaka, J. Chem. Phys. **122**, 104711 (2005).
[10] J. Bai, C. A. Angell, and X. C. Zeng, Proc. Natl. Acad. Sci. U.S.A. **107**, 5718 (2010).
[11] K. B. Jinesh and J. W. M. Frenken, Phys. Rev. Lett. **101**, 036101 (2008).
[12] E. M. Choi, Y. H. Yoon, S. Lee, and H. Kang, Phys. Rev. Lett. **95**, 085701 (2005).
[13] R. Zangi and A. E. Mark, J. Chem. Phys. **120**, 7123 (2004).
[14] X. Xia and M. L. Berkowitz, Phys. Rev. Lett. **74**, 3193 (1995).
[15] D. Ehre, E. Lavert, M. Lahav, and I. Lubomirsky, Science **327**, 672 (2010).
[16] J. L. Aragones, L. G. MacDowell, J. I. Siepmann, and C. Vega, Phys. Rev. Lett. **107**, 155702 (2011).
[17] M. W. Mahoney and W. L. Jorgensen, J. Chem. Phys. **112**, 8910 (2000).
[18] A. M. Saitta, F. Saija, and P. V. Giaquinta, Phys. Rev. Lett. **108**, 207801 (2012).
[19] See Supplemental Material at http://link.aps.org/supplemental/10.1103/PhysRevLett.110.195701 for density functional theory calculation results for water dissociation, calculated pressure change with respect to the field strength, and simulation results with the TIP4P water model.
[20] B. Hess, C. Kutzner, D. van der Spoel, and E. Lindahl, J. Chem. Theory Comput. **4**, 435 (2008).
[21] H. J. C. Berendsen, J. P. M. Postma, W. F. van Gunsteren, A. DiNola, and J. R. Haak, J. Chem. Phys. **81**, 3684 (1984).
[22] W. Drost-Hansen and J. Lin Singleton, *Fundamentals of Medical Cell Biology* (JAI, Greenwich, CT, 1992), Vol. 3a, p. 157.
[23] M. Gavish, J. L. Wang, M. Eisenstein, M. Lahav, and L. Leiserowitz, Science **256**, 815 (1992).
[24] S. H. Khan, G. Matei, S. Patil, and P. M. Hoffmann, Phys. Rev. Lett. **105**, 106101 (2010).
[25] Under an extremely high electric field (e.g., 50 V/nm), the system transforms to a highly ordered crystal-like structure, as indicated by the low lateral diffusion coefficient in Fig. 1; the strong positional restriction in Figs. 2(a), 2(b), and 2(d); the strong orientation polarization in the inset of Fig. 2(d); the virtually zero value of the intraplane H-bond number in Fig. 3(b); and the slow decay of H-bond lifetime in Fig. 3(c). This alignment was suggested to be energetically the most favorable configuration of water molecules under extremely high electric fields [5,6].
[26] W. L. Jorgensen and J. D. Madura, Mol. Phys. **56**, 1381 (1985).